

Removal of heavy metal ions from aqueous solution by zeolite synthesized from fly ash

Kuang He¹ · Yuancai Chen¹ · Zhenghua Tang¹ · Yongyou Hu¹

Received: 25 June 2015 / Accepted: 14 September 2015 / Published online: 8 October 2015
© Springer-Verlag Berlin Heidelberg 2015

Abstract Zeolite was synthesized from coal fly ash by a fusion method and was used for the removal of heavy metal ions (Pb^{2+} , Cd^{2+} , Cu^{2+} , Ni^{2+} , and Mn^{2+}) in aqueous solutions. Batch method was employed to study the influential parameters such as adsorbent dosage, pH, and coexisting cations. Adsorption isotherms and kinetics studies were carried out in single-heavy and multiheavy metal systems, respectively. The Langmuir isotherm model fitted to the equilibrium data better than the Freundlich model did, and the kinetics of the adsorption were well described by the pseudo-second-order model, except for Cd^{2+} and Ni^{2+} ions which were fitted for the pseudo-first-order model in the multiheavy metal system. The maximum adsorption capacity and the distribution coefficients exhibited the same sequence for $\text{Pb}^{2+} > \text{Cu}^{2+} > \text{Cd}^{2+} > \text{Ni}^{2+} > \text{Mn}^{2+}$ in both single- and multiheavy metal systems. In the end, the adsorption capacity of zeolite was tested using industrial wastewaters and the results demonstrated that zeolite could be used as an alternative adsorbent for the removal of heavy metal ions from industrial wastewater.

Keywords Fly ash · Zeolite · Adsorption · Heavy metals

Abbreviations

| | |
|-------|-------------------------------------|
| XRF | X-ray fluorescence |
| XRD | X-ray diffraction |
| SEM | Scanning electron microscope |
| BET | Brunauer Emmet teller |
| FTIR | Fourier transform infrared |
| AAS | Atomic adsorption spectrophotometer |
| CEC | Cation exchange capacity |
| LOI | Loss on ignition |
| R | Removal efficiency |
| K_d | Distribution coefficients |
| R^2 | correlation coefficients |

Introduction

Several industrial wastewaters may contain heavy metals. These toxic metals, if not properly disposed, can be severely harmful to human health and the environment (Balsamo et al. 2011; Bayat 2002; Hui et al. 2005; Shi et al. 2013). Various methods for the removal of heavy metals have been carried out, such as chemical precipitation, solvent extraction, ion exchange, reverse osmosis or adsorption, and so on (Fu and Wang 2011; Mohan and Gandhinathi 2009; Yadav et al. 2013). Among these methods, adsorption has been proven to be an effective technique due to its great efficiency and simplicity in operation as well as its incredible versatility (Xu et al. 2013). The most commonly used adsorbents for heavy metal removal are activated carbon, alumina, and silica (Barczak et al. 2015; Fu and Wang 2011; Karnib et al.

Responsible editor: Philippe Garrigues

✉ Yuancai Chen
chenyc@scut.edu.cn

¹ Ministry of Education Key Laboratory of Pollution Control and Ecological Remediation for Industrial Agglomeration Area, State Key Laboratory of Pulp and Paper Engineering, New Energy Research Institute, School of Environment and Energy, South China University of Technology, Guangzhou Higher Education Mega Center, Guangzhou 510006, People's Republic of China

2014). But, the relatively high costs significantly limited their application, especially for developing countries and regions (Boujelben et al. 2009). Therefore, searching for alternative low-cost adsorbents for the removal of heavy metal ions is highly desired. Recently, a variety of low-cost adsorbents have been developed and tested to remove heavy metal ions from aqueous solutions, including clay minerals (Franus et al. 2014), bioadsorbents (Ajjabi and Chouba 2009), zeolites (Álvarez-Ayuso et al. 2003; Hui et al. 2005; Kyziol-Komosinska et al. 2015), and industrial by-products (Fu and Wang 2011).

Fly ash, one of the major industrial solid wastes, is generated during the combustion of coal for energy production (Wang et al. 2008). The chemical components of fly ash are mainly alumina, silica, and calcium oxide. The characteristic physical features of fly ash, including bulk density, porosity, and surface, make it an economical alternative for conventional adsorbents. However, fly ash still shows lower adsorption capacity compared with that of the traditional adsorbent (Ahmaruzzaman 2010). Therefore, the adsorption capacity of fly ash has been improved by different activation methods (Izidoro et al. 2013). Among these methods, conversion of fly ash to crystalline zeolites has been gaining much attention during the past years (Li et al. 2006; Wang et al. 2007; Querol et al. 2001). Zeolites are microporous, hydrated, crystalline aluminosilicates characterized by a three-dimensional network of tetrahedrons [AlO_4] and [SiO_4] connected by their corners (Álvarez-Ayuso et al. 2003). The zeolite's structure is characterized by a regular system of channels and chambers which bring a large adsorption capacity (Bandura et al. 2015; Zhan et al. 2013). Since Höller and Wrisching (1985) firstly synthesized zeolites from fly ash; many patents and technical articles have proposed different methods for the synthesis of different zeolites from fly ash (Franus et al. 2014; Izidoro et al. 2013; Li et al. 2006; Wdowin et al. 2014). Hydrothermal process is the most common method, whereby the fly ash is mixed with alkaline solution at different conditions of temperature, pressure, and reaction time (Bukhari et al. 2015). However, zeolites synthesized by this method still contain a significant amount of residual fly ash (Hollman et al. 1999). Shigemoto et al. proposed a fusion method by introducing a fusion step prior to the hydrothermal treatment, which made alkali extract more silicates and aluminates from fly ash and increase the yield of zeolites (Izidoro et al. 2013; Shigemoto et al. 1995). Thus, a fusion method was used for the synthesis of zeolite in this study.

Several researches have studied the removal of heavy metal ions using zeolites synthesized from fly ash. Wu et al. (2008) synthesized zeolites from different fly ashes and utilized these in the removal of Cr^{3+} from aqueous solution. The synthesized zeolites showed a much greater ability than fly ash did for the

removal of Cr^{3+} ions. Álvarez-Ayuso et al. (2003) studied the adsorption various toxic metal ions (Cr^{3+} , Ni^{2+} , Zn^{2+} , Cu^{2+} , and Cd^{2+}) on natural and synthetic zeolite. The synthetic zeolite showed much higher adsorption capacity for all the ions than did the natural zeolite. Izidoro et al. (2013) synthesized zeolites from fly ash and used these in the adsorption of Zn^{2+} and Cd^{2+} ions; the results showed that the adsorption capacities for Zn^{2+} and Cd^{2+} were ranged from 156 to 220 and 57 to 195 mg/g in the single and binary ion systems, respectively. Hui et al. (2005) reported that synthetic zeolite 4A showed good adsorptive properties on the treatment of mixed metal effluents; the maximum adsorption capacity for Co^{2+} , Cr^{3+} , Cu^{2+} , Ni^{2+} , and Zn^{2+} was 13.72, 41.61, 50.45, 8.69, and 30.80 mg/g, respectively. The results have demonstrated that zeolites have a good ability to remove heavy metals from aqueous solution. The general observation is that most of the studies on the adsorption of metal ions have been devoted to a single metal system. However, industrial wastewaters usually contained several heavy metal ions (Padervand and Gholami 2013; Prakash et al. 2012). Conclusions drawn from these studies may not be valid for the multiheavy metal system.

The main goal of this work was to synthesize zeolite from fly ash and investigate its adsorption capacity of heavy metal ions (Pb^{2+} , Cu^{2+} , Cd^{2+} , Ni^{2+} , and Mn^{2+}) in both single-heavy and multiheavy metal systems. The influence of dosage, pH, and coexisting ions were also elucidated. In addition, the selectivity sequences of adsorption of these metal ions in the zeolite were established by means of distribution coefficients (Covelo et al. 2004). Finally, the effectiveness of zeolite for the removal of heavy metal ions was evaluated using industrial wastewaters, including desulfurization wastewater from a wet limestone-gypsum system and metal plating wastewater from local metal plating factory.

Materials and methods

Materials and chemicals

The fly ash used in this study was collected from a thermal power plant in Zhanjiang, China. The chemical composition of fly ash was given in Table 1. According to the American Association for Testing and Materials (ASTM C618), the fly ash used in this study can be classified as class F (Ahmaruzzaman 2010). All chemicals used in this study were of analytical grade.

Synthesis of zeolite

Fly ash was screened with a 200-mesh sieve in order to remove impurities. To enhance the zeolitization, a fusion

Table 1 The chemical composition of fly ash

| Compound | Weight (%) |
|--------------------------------|------------|
| SiO ₂ | 49.8 |
| Al ₂ O ₃ | 39.7 |
| Fe ₂ O ₃ | 3.1 |
| CaO | 2.3 |
| TiO ₂ | 1.4 |
| MgO | 0.3 |
| K ₂ O | 0.2 |
| LOI | 3.2 |

method was used in this study to synthesize zeolite from fly ash (Izidoro et al. 2013; Somerset et al. 2005). The method took a two-step process. In the first step, 10 g of fly ash was mixed and ground with 12 g of NaOH to obtain a homogeneous mixture. The mixture was then heated at 550 °C for 1 h. Secondly, the mixture was ground and dissolved in 85 mL of distilled water and stirred at room temperature for 24 h. The mixture was then heated to 105 °C in an oven for hydrothermal synthesis for 24 h. After cooling to room temperature, the mixture was filtered and the solid was washed several times with distilled water and then dried overnight at 105 °C.

Characterization methods

The samples were characterized using several techniques. The chemical composition of fly ash was determined by X-ray fluorescence (XRF, PANalytical PW4400, Netherlands). X-ray diffraction (XRD) analysis was performed using a diffractometer (Bruker-D8 ADVANCE, Germany), where samples were exposed to X-ray ($k=1.5418 \text{ \AA}$) with the 2θ angle varying between 5° and 80° with Cu K α radiation. The surface morphology of the fly ash and zeolite was visualized using a scanning electron microscope (SEM, ZEISS Merlin, Germany). The specific surface areas of the zeolite samples were determined by the Brunauer Emmet Teller method (BET, Quantachrome NOVA 4200e, USA). Prior to determination of the specific surface area, samples were heated at 200 °C for 4 h to remove volatiles and moisture in a degasser (Quantachrome NOVA 4200e, USA) and the analyses were carried out at -196 °C with nitrogen. The BET surface areas were obtained by applying the equation to the nitrogen adsorption data. Fourier transform infrared (FTIR, Nicolet Continuum, USA) spectra of fly ash and zeolite were acquired with a Vector 33 with KBr discs. The loss on ignition (LOI) was determined by heating the pre-weighed dry fly ash to 800 °C over a period of 2 h. Cation exchange capacity (CEC) values of the fly ash and zeolite were determined using a modified ammonium acetate method. In the CEC measurements, samples were saturated in ammonium acetate solution (1 M) and the sodium ion concentration of the resulting

solution was determined by an Atomic Adsorption Spectrophotometer (AAS, PerkinElmer PinAAcle 900T, USA).

Adsorption experiments

In order to study the effect of different influential parameters such as adsorbent dosage, pH, and coexisting ions, batch experiments were conducted with 100 mL of solutions in 250 mL conical flasks and shaken in shaking incubators (Zhicheng ZWYR-2102C, China) at 150 rpm. The solutions were prepared from the stock solution of 2000 mg/L, and the pH of the solutions was adjusted using HNO₃ or NaOH solutions. All experiments were carried out at 30 °C, and the separation of solutions and adsorbent particles was achieved by filtration through 0.45- μm membrane filters. The concentrations of the heavy metal ions were determined by AAS (PerkinElmer PinAAcle 900T, USA).

Adsorption kinetics and isotherms of heavy metals in single and multiple systems

For the adsorption experiments of isotherms and kinetics, the zeolite dosage was constant at 1 g/L with the pH of 5.0. The kinetics of the adsorption was studied by mixing the zeolite with heavy metals in single-heavy and multiheavy metal systems with the initial concentration of 100 mg/L. The solutions were shaken from 5 to 240 min to investigate the adsorption kinetics. Batch experiments were also carried out by mixing the zeolite with different amounts of heavy metals in single and multiple systems, and the solutions were shaken for 4 h to construct the adsorption isotherms.

The removal efficiency (R) and adsorption capacity (q) were calculated using the following equations:

$$R = \frac{C_0 - C_1}{C_0} \times 100\% \quad (1)$$

$$q = \frac{(C_0 - C_1)V}{m} \quad (2)$$

where C_0 is the initial concentration of heavy metal ions and C_1 is the residual concentration of metal ions; V is the volume of solution (l); and m is the mass of the adsorbent (g).

Results and discussion

Characterization of fly ash and zeolite

The XRD patterns of fly ash and zeolite are presented in Fig. 1. The phases were identified by comparing the peak positions and intensities with those in the JCPDS data files. As can be seen in Fig. 1, fly ash has several characteristic

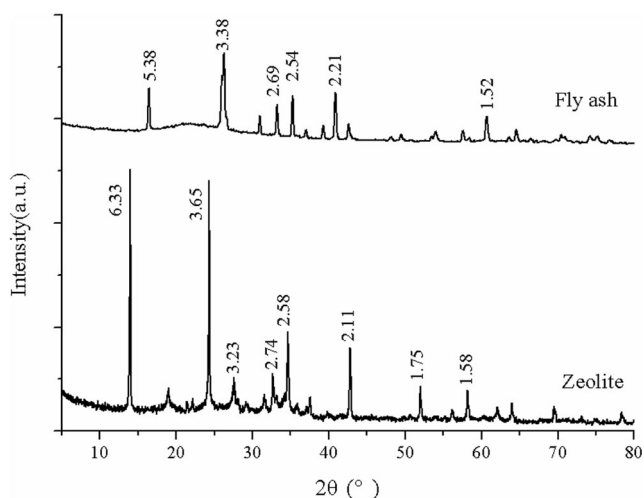


Fig. 1 The XRD patterns of fly ash and zeolite

peaks (5.38, 3.38, 2.69, 2.54, 2.21, and 1.52 Å); according to the XRD pattern, these peaks are identified as mullite (JCPDS card 06-0258). In contrast to the fly ash XRD pattern, the synthesized zeolite is different. The crystalline phases of mullite disappeared and some new peaks appeared (6.33, 3.65, 3.23, 2.74, 2.58, 2.11, 1.75, and 1.58 Å), which were identified as sodalite (JCPDS card 31-1270).

Figure 2 shows the FTIR spectra of fly ash and zeolite. The major bands for fly ash can be assigned as follows: 3414 cm^{-1} (–OH stretching vibration), 1634 cm^{-1} (O–H bending), 1098 cm^{-1} (Si–O–Si or Al–O–Si asymmetric stretching), 890 cm^{-1} (Si–O–Si or Al–O–Si symmetric stretching), and 461 and 559 cm^{-1} (stretching vibration of Al–O–Al) (Álvarez-Ayuso et al. 2008). Synthesized process could cause the change of the infrared spectra. The band at about 461 and 1098 cm^{-1} was shifted to lower frequencies about 435 and 986 cm^{-1} , respectively. However, the band at around

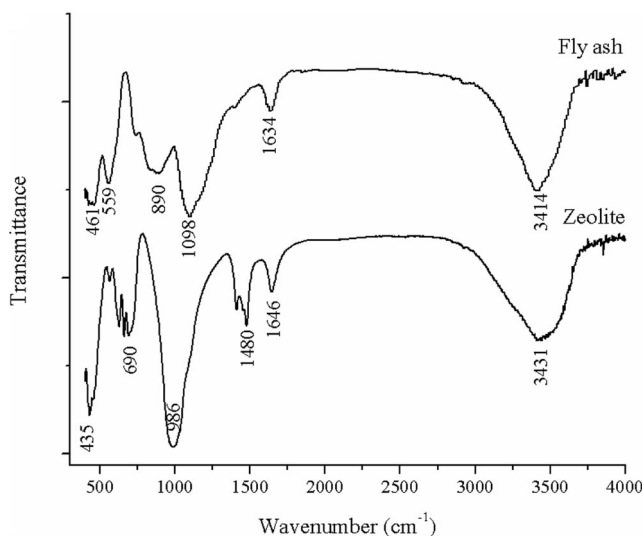


Fig. 2 FTIR spectra of fly ash and zeolite

3414 cm^{-1} was shifted to higher frequencies and the intensity of the band was decreased (Huang and Han 2011). The bands at around 559 and 890 cm^{-1} disappeared and new some peaks appeared at around 690 cm^{-1} which were associated with Si–O–Si and Al–O–Si symmetric stretching. The spectra bands at about 1480 cm^{-1} appeared in the zeolite sample, which is the characteristic of carbonate asymmetric stretching. The presence of sodium carbonate might be due to the atmospheric carbonation of alkaline activation media (Álvarez-Ayuso et al. 2008).

Figure 3 illustrates the morphological features of the fly ash and the synthesized zeolite. As shown in Fig. 3a, fly ash has particles of various shapes with a relatively smooth surface, including spheres and agglomerates. After alkaline fusion and hydrothermal treatment, as is shown in Fig. 3b, the spheres and agglomerates have changed to various crystal shapes and the particle size have become much smaller. The specific surface area of the materials increased from 7.5 to 12.7 m^2/g , which was due to the porosity development within the zeolitization process. In addition, the obtained CEC values of zeolite and fly ash increased from 0.03 to 1.64 meq/g. The results indicated the enhanced capacity of zeolite for removing heavy metals in aqueous solutions.

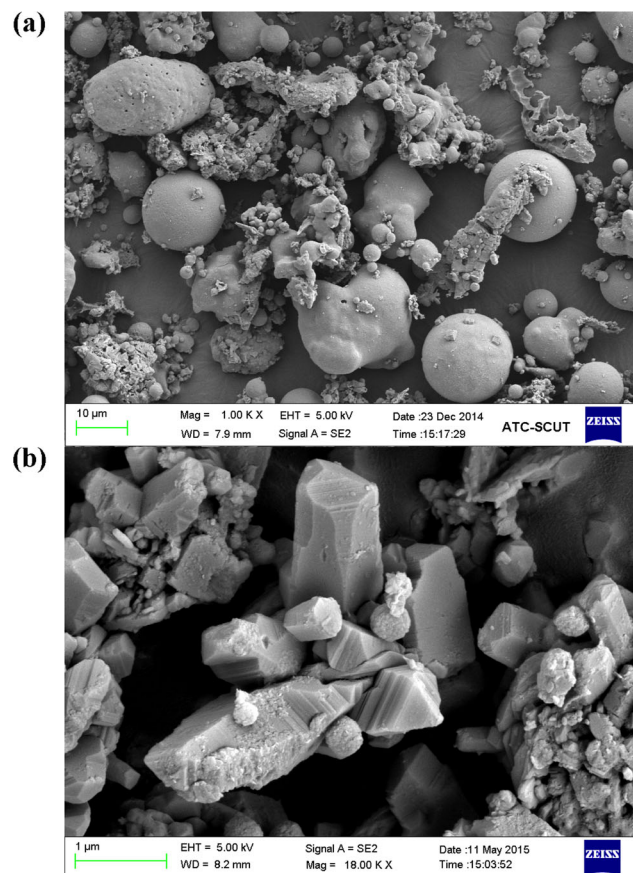


Fig. 3 The SEM images of fly ash (a) and zeolite (b)

Parameters affecting heavy metals' adsorption

Effect of adsorbent dosage

The effects of the zeolite and fly ash dosages on the removal of heavy metals in multiple systems with the initial concentration of 100 mg/L were shown in Fig. 4. It is noted that removal efficiencies of heavy metals increased with the increase of dosage for synthesized zeolite and fly ash. At any specific dosage, synthesized zeolite achieved higher performance than did fly ash. The removal efficiency increased from 51 to 99 % for Pb^{2+} , 30 to 94 % for Cu^{2+} , 22 to 86 % for Cd^{2+} , 10 to 50 % for Ni^{2+} , and 7 to 35 % for Mn^{2+} as the zeolite dosage increases from 1 to 5 g/L. As the zeolite dosage exceeds 10 g/L, over 95 % of the metal ions were removed for Pb^{2+} , Cu^{2+} , and Cd^{2+} , and over 80 % of the metal ions were removed for Ni^{2+} and Mn^{2+} , respectively. In contrast, fly ash presented a much

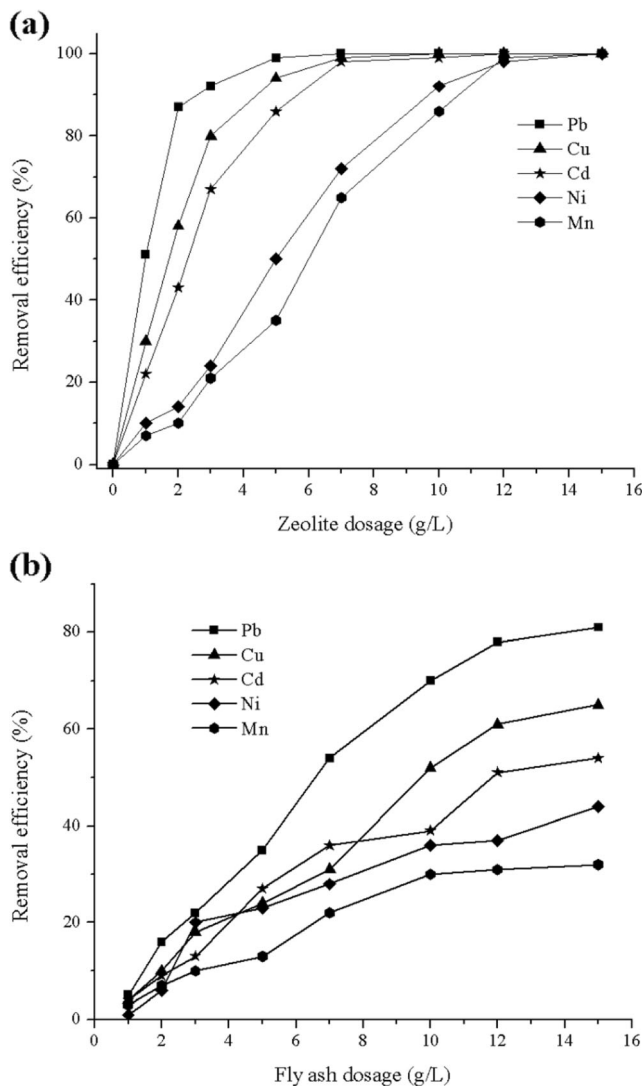


Fig. 4 Effect of zeolite and fly ash dosage on the removal of heavy metals

lower adsorption capacity for heavy metals than zeolite did, as shown in Fig. 4b. The removal efficiency was only 81, 65, 54, 44, and 32 % for Pb^{2+} , Cu^{2+} , Cd^{2+} , Ni^{2+} , and Mn^{2+} , respectively, when the fly ash dosage was 15 g/L. The significantly enhanced removal efficiency of zeolite appeared to be attributed to the higher CEC value, the larger surface area, and the smaller particle size after synthesis, and the corresponding increase of the available adsorption sites as a result of the increased adsorbent dosage (Wang et al. 2007; Xu et al. 2010).

Effect of pH

Effects of pH on the adsorption of heavy metal ions by the synthesized zeolite at pH 1.0–12.0 were shown in Fig. 5. Experiments were conducted with a zeolite dosage of 5 g/L and an initial concentration of 100 mg/L. The removal efficiency was less than 10 % for all metal ions when the solution pH was 1.0, and it increased rapidly as the pH increased from 1.0 to 5.0. The removal efficiency was 99, 98, 93, 80, and 63 % for Pb^{2+} , Cu^{2+} , Cd^{2+} , Ni^{2+} , and Mn^{2+} ions, respectively, when the initial pH of the solution was 5.0. The low removal efficiency of metal ions at lower pH can be due to the competition between H_3O^+ and metal ions and the increase in positive charge of the zeolite surface. In addition, the hydroxyl groups (Si-OH and Al-OH) on the adsorbent surface can be ionized in aqueous solution (Cho et al. 2005). As the pH increased, it could enhance the dissociation of the hydroxyl groups, leaving more anionic sites and making a significant contribution to the adsorption of metal ions. Furthermore, the pH for precipitation at the concentration of 100 mg/L was 5.7, 5.8, 8.6, 7.7, and 8.7 for Pb^{2+} , Cu^{2+} , Cd^{2+} , Ni^{2+} , and Mn^{2+} , respectively, based on the solubility products of the metal hydroxides, indicating that the removal of the metals was mainly accomplished by adsorption at a pH lower than 5.0. At higher pH values (>8.7), heavy metal hydroxides were the main species, and the metal ions were removed via a precipitation process.

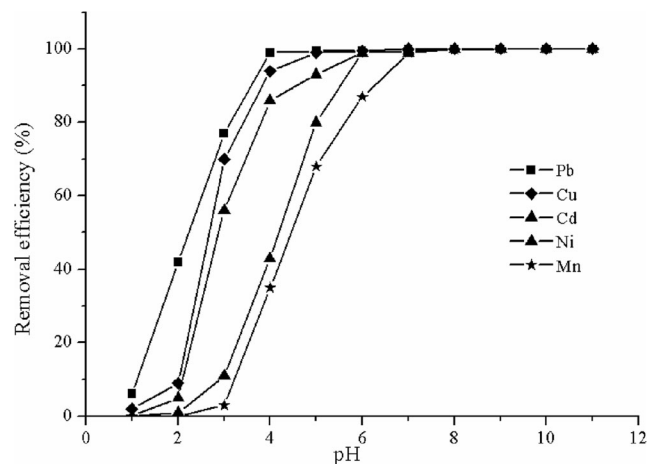


Fig. 5 Effect of initial pH on the removal efficiency

Effect of coexisting cations

The coexisting cations in aqueous solution could compete with heavy metal ions for the adsorption sites on the adsorbent (Wen et al. 2011). In this study, the individual effects of coexisting cations, such as Al^{3+} , Ca^{2+} , Mg^{2+} , Na^+ , and NH_4^+ that are usually present in aqueous solution were investigated with the concentration of 0.1 M. Blank experiments were also conducted without coexisting cations. The experiments were carried out at initial heavy metal ions of 100 mg/L, initial solution pH 5.0, and zeolite dosage of 10 g/L, and the results were shown in Fig. 6. The removal efficiency of heavy metals was reduced significantly with the presence of coexisting cations. The reduction tendency which clearly demonstrated the effect of the cations was in the order of $Al^{3+} > NH_4^+ > Ca^{2+} > Mg^{2+} > Na^+$. The competition capacity of coexisting metal cations might be determined by the electric charge and the ionic radii of the ions (Vega et al. 2006). In addition, the complex interaction between heavy metals and NH_4^+ also affects the adsorption capacity of heavy metals.

Adsorption kinetics in single-heavy and multiheavy metal systems

The dynamics of adsorption describes the rate of solute uptake, which in turn governs the duration time of the adsorption reaction. Pseudo-first-order and pseudo-second-order reaction models were employed to fit the experimental data, as expressed by the following equations (Ayoob et al. 2008; Hui et al. 2005):

$$\log(qe - qt) = \log qe - \frac{K1}{2.303} t \tag{3}$$

$$\frac{t}{qt} = \frac{1}{K_2 q_e^2} + \frac{t}{q_e} \tag{4}$$

where q_e and q_t (mg/g) are the amounts of heavy metal ions adsorbed onto the adsorbent at equilibrium and at time t (min),

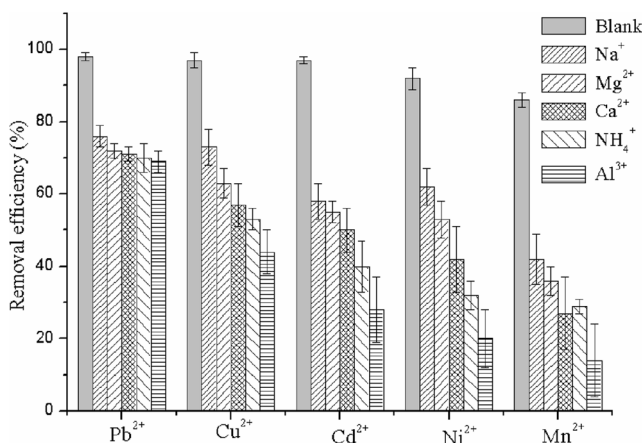


Fig. 6 Effect of coexisting ions on the removal efficiency

respectively. The adsorption rate constant K_1 was calculated from the slope of the linear plot $\log(q_e - q)$ versus time t and the rate constant K_2 can be determined from the intercept.

Adsorption kinetics of the heavy metals in single and multiple systems on the adsorbent was depicted in Fig. 7, and the kinetic parameters were listed in Table 2. It can be seen that most adsorption which took place at the first 60 and 240 min was enough for the adsorption to reach equilibrium. Therefore 240 min was fixed as the contact time for other experiments. In the single heavy metal system, the high correlation coefficient ($R^2 > 0.97$) and the good agreement of calculated and experimental data confirm that adsorption processes followed the pseudo-second-order kinetics.

In the multiple metal systems, The R^2 of the pseudo-first-order model for Pb^{2+} , Cu^{2+} , Cd^{2+} , Ni^{2+} , and Mn^{2+} were 0.966, 0.971, 0.979, 0.998, and 0.942, and the R^2 of the pseudo-second-order model for Pb^{2+} , Cu^{2+} , Cd^{2+} , Ni^{2+} , and Mn^{2+} were 0.970, 0.992, 0.907, 0.969, and 0.988 respectively. The results indicated that the pseudo-first-order model fitted better for the adsorption of Cd^{2+} and Ni^{2+} ions and the pseudo-

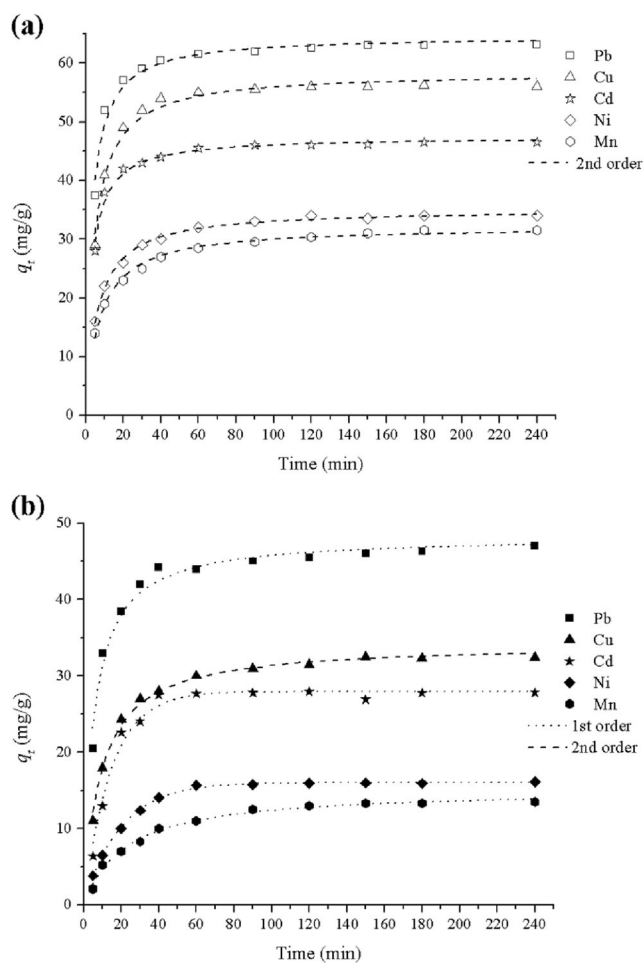


Fig. 7 Kinetics of heavy metals in single and multiple systems: a single system, b multiple system. (1st order, pseudo-first-order model; 2nd order, pseudo-second-order model)

Table 2 Kinetics parameters obtained from the adsorption of heavy metals in single and multiple systems

| System | Metal ions | Pseudo-first-order | | | Pseudo-second-order | | |
|-----------------|------------------|--------------------|---------------|-------|---------------------|--------------------|-------|
| | | q_e (mg/g) | K_1 (1/min) | R^2 | q_e (mg/g) | K_2 (g/(mg×min)) | R^2 |
| Single system | Pb ²⁺ | 61.6 | 0.182 | 0.955 | 64.6 | 0.0051 | 0.971 |
| | Cu ²⁺ | 55.1 | 0.136 | 0.971 | 58.4 | 0.0038 | 0.981 |
| | Cd ²⁺ | 45.3 | 0.184 | 0.943 | 47.5 | 0.0069 | 0.978 |
| | Ni ²⁺ | 32.6 | 0.106 | 0.900 | 35.0 | 0.0046 | 0.995 |
| | Mn ²⁺ | 29.7 | 0.099 | 0.876 | 32.1 | 0.0043 | 0.990 |
| Multiple system | Pb ²⁺ | 45.1 | 0.118 | 0.966 | 48.2 | 0.0038 | 0.970 |
| | Cu ²⁺ | 31.3 | 0.076 | 0.971 | 34.2 | 0.0032 | 0.992 |
| | Cd ²⁺ | 27.9 | 0.069 | 0.979 | 30.6 | 0.0031 | 0.907 |
| | Ni ²⁺ | 16.1 | 0.051 | 0.998 | 17.9 | 0.0038 | 0.969 |
| | Mn ²⁺ | 13.0 | 0.048 | 0.942 | 15.2 | 0.0029 | 0.988 |

second-order model fitted better for the adsorption of Pb²⁺, Cu²⁺, and Mn²⁺ ions. Moreover, the adsorption rate constants of the pseudo-second-order model in the single system were higher than that in the multiheavy metal system for all of the five heavy metals, suggesting that the adsorption of heavy metals in the single heavy metal system was faster than in that in the multiheavy metal system in reaching adsorption equilibrium. The differences of adsorption kinetics and rate constants between the single and multiple systems were affected by the interaction and competition effects among the multiheavy metal ions.

Adsorption isotherms of heavy metals in single-heavy and multiheavy metal systems

The adsorption study of the interaction between heavy metals and the adsorbent can be well described by the two most classic isotherm models, namely Langmuir (Wu et al. 2008) and Freundlich (Ahmaruzzaman 2010). Langmuir isotherm is applicable to the monolayer and homogeneous adsorption, while Freundlich isotherm is an empirical model applicable to adsorption onto heterogeneous surfaces. The Langmuir and Freundlich isotherm models are given in Eqs. (5) and (6), respectively.

$$q_e = \frac{q_m K C_e}{1 + K C_e} \quad (5)$$

$$q_e = K_f C_e^{1/n} \quad (6)$$

where C_e is the equilibrium concentration of heavy metal ions (mg/L), q_m is the theoretical maximum adsorption capacity (mg/g), and K represents the Langmuir equilibrium constant (L/mg). K_f ((mg/g)/(mg/L)^{1/n}) is the Freundlich constant which represents the adsorption capacity when the heavy metal ion equilibrium concentration equals to 1. The value of n gives an indication of the favorability of adsorption.

The adsorption isotherms of heavy metals in single and multiple systems were shown in Fig. 8. The isotherm

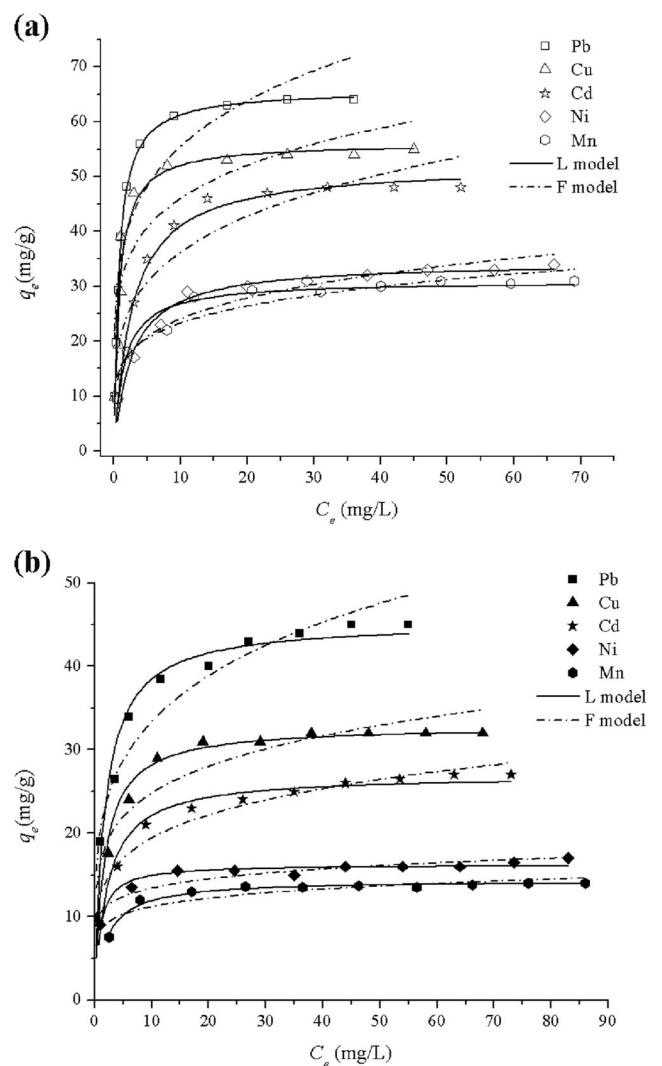


Fig. 8 Adsorption isotherms of heavy metals in single and multisystem: **a** single system, **b** multiple system. *L* Langmuir, *F* Freundlich)

Table 3 Isotherm parameters obtained from the adsorption of heavy metals in single and mixed systems

| System | Metal ions | Langmuir model | | | Freundlich model | | |
|---------------|------------------|----------------|------------|-------|--|------|-------|
| | | q_m (mg/g) | K (L/mg) | R^2 | $K_f((\text{mg/g})/(\text{mg/L})^{1/n})$ | n | R^2 |
| Single system | Pb ²⁺ | 65.75 | 1.371 | 0.995 | 34.91 | 4.90 | 0.837 |
| | Cu ²⁺ | 56.06 | 1.303 | 0.937 | 30.61 | 5.65 | 0.779 |
| | Cd ²⁺ | 52.12 | 0.367 | 0.969 | 21.04 | 4.24 | 0.856 |
| | Ni ²⁺ | 34.40 | 0.377 | 0.953 | 14.85 | 4.76 | 0.914 |
| | Mn ²⁺ | 30.89 | 0.668 | 0.946 | 15.36 | 5.52 | 0.866 |
| Mixed system | Pb ²⁺ | 45.28 | 0.563 | 0.968 | 20.15 | 4.56 | 0.927 |
| | Cu ²⁺ | 32.86 | 0.603 | 0.938 | 16.65 | 5.68 | 0.882 |
| | Cd ²⁺ | 26.93 | 0.459 | 0.947 | 12.51 | 5.23 | 0.943 |
| | Ni ²⁺ | 16.25 | 1.137 | 0.938 | 10.34 | 8.85 | 0.866 |
| | Mn ²⁺ | 14.63 | 0.491 | 0.976 | 8.41 | 8.06 | 0.745 |

parameters were listed in Table 3. As shown in Table 3, the R^2 of the Langmuir model was higher than that of the Freundlich model for all cases, indicating that the Langmuir model represents a better fit to the experimental data. The good agreement of the Langmuir model with the experimental data indicates monolayer coverage of the heavy metals on the surface of zeolite. The maximum equilibrium adsorption capacity (q_m) for Pb²⁺, Cu²⁺, Cd²⁺, Ni²⁺, and Mn²⁺ ions was 65.75, 56.06, 52.12, 34.40, and 30.89 mg/g in the single system, which exhibited the same sequence and decreased to 45.28, 32.86, 26.93, and 16.25 mg/g in the multiheavy metal system. It was found that the amount of adsorbent metals in the single system was larger than that of the multiheavy metal system; this might be due to the competition of the metal ions for the adsorption sites. In addition, the adsorption of Pb²⁺ ions was higher than that of other metal ions in both single-heavy and multiheavy metal systems. Similar results have been reported in other studies (Mohan and Gandhinathi 2009; Sprynskyy et al. 2006; Inglezakis et al. 2002).

In addition, the distribution coefficient (K_d) was used to evaluate the selectivity sequence of the heavy metals in this study and was calculated using the following equation (Covelo et al. 2004):

$$K_d = \frac{q_e}{C_e} \tag{7}$$

The distribution coefficients of the single system (K_{ds}) and the multiple system (K_{dm}) were tested with the initial concentrations of the heavy metals of 50 and 100 mg/L, respectively. The values were shown in Table 4. The result indicates that the selectivity sequence of metal ions onto zeolite is Pb²⁺ > Cu²⁺ > Cd²⁺ > Ni²⁺ > Mn²⁺.

Many parameters may be responsible for the observed selectivity, such as the characteristics of zeolites and heavy metal ions (Hui et al. 2005; Mihaly-Cozmuta et al. 2014). Generally, zeolites are weakly acidic in nature and, therefore, sodium form exchangers are selective for hydrogen. This leads to high pH values of the solutions, making feasible the metal hydroxide precipitation (Leinonen and Lehto 2001). The characteristics of heavy metal ions, such as hydrolysis constant, dehydration energy, and hydrated radii, were summarized in Table 5 (Hui et al. 2005; Mihaly-Cozmuta et al. 2014; Semmens and Seyfarth 1978; Volkov et al. 1997). The metal ions with higher dehydration energy, hydrolysis constant, and larger hydrated radii were preferred to remain in the solution phase. According to the values of the hydrolysis constant, the selectivity of the metal ions was Cu²⁺ > Pb²⁺ > Cd²⁺ > Ni²⁺ > Mn²⁺. The dehydration energy of heavy metal ions indicated that the selectivity sequence of the metal ions was as follows: Pb²⁺ > Cd²⁺ > Mn²⁺ > Cu²⁺ > Ni²⁺. Also, according to the size of the hydrated radii of metal ions from the Table 5, the selectivity sequence was Pb²⁺ > Ni²⁺ > Cu²⁺ >

Table 4 Distribution coefficients of heavy metals in single and mixed system

| Metal ions | K_{dm} (L/g) 50 mg/L | K_{ds} (L/g) | K_{dm}/K_{ds} | K_{dm} (L/g) 100 mg/L | K_{ds} (L/g) | K_{dm}/K_{ds} |
|------------------|------------------------|----------------|-----------------|-------------------------|----------------|-----------------|
| Pb ²⁺ | 3.35 | 25.31 | 0.132 | 0.82 | 1.77 | 0.460 |
| Cu ²⁺ | 1.63 | 15.67 | 0.104 | 0.47 | 1.22 | 0.385 |
| Cd ²⁺ | 0.92 | 4.55 | 0.202 | 0.37 | 0.92 | 0.400 |
| Ni ²⁺ | 0.42 | 1.5 | 0.285 | 0.20 | 0.51 | 0.397 |
| Mn ²⁺ | 0.37 | 1.42 | 0.261 | 0.16 | 0.45 | 0.362 |

Table 5 Properties of different metal ions

| Metal ions | Hydrated radii (nm) | Dehydration energy (kJ/mol) | Hydrolysis constant pK_1 |
|------------------|---------------------|-----------------------------|----------------------------|
| Pb ²⁺ | 0.401 | 1480 | 7.8 |
| Cu ²⁺ | 0.419 | 2100 | 7.34 |
| Cd ²⁺ | 0.426 | 1806 | 9.2 |
| Ni ²⁺ | 0.404 | 2106 | 9.86 |
| Mn ²⁺ | 0.438 | 1845 | 10.59 |

Cd²⁺ > Mn²⁺. The selectivity sequence according to the hydrolysis constant explains well the observed sequence, which indicated that the hydrolysis constant was the main parameter which affects the adsorption of heavy metals. In addition, zeolites have a higher preference for Pb²⁺ ions than Cu²⁺ ions. This happens probably because Pb²⁺ has lower dehydration energy and smaller hydrated radii.

Several selectivity sequences have been reported in the literature for different adsorbent: for fly ash, Pb²⁺ > Cd²⁺ > Zn²⁺ > Cu²⁺ > Mn²⁺ (Mohan and Gandhinathi 2009); for clinoptilolite, Pb²⁺ > Cu²⁺ > Zn²⁺ (Calvo et al. 2009), Pb²⁺ > Cu²⁺ > Cd²⁺ > Zn²⁺ > Cr³⁺ > Co²⁺ > Ni²⁺ (Ouki and Kavannagh 1997), Pb²⁺ > Cu²⁺ > Cd²⁺ > Ni²⁺ (Sprynskyy et al. 2006); for NaP1, Cr³⁺ > Cu²⁺ > Zn²⁺ > Cd²⁺ > Ni²⁺ (Álvarez-Ayuso et al. 2003); and for zeolite 4A, Cu²⁺ > Co²⁺ > Mn²⁺ > Zn²⁺ > Cd²⁺ > Ni²⁺ (Majdan et al. 2003), Cu²⁺ > Cr³⁺ > Zn²⁺ > Co²⁺ > Ni²⁺ (Hui et al. 2005). In general, zeolites have a higher preference for Pb²⁺ and Cu²⁺ than for Cd²⁺, Ni²⁺, and Mn²⁺ ions, which were consistent with the conclusion in this study. Moreover, the observed differences might be due to the differences of the adsorbent properties and the techniques used in the experiments.

To study the competition of the metal ions, the values of K_{dm}/K_{ds} were calculated and listed in Table 4. The values of K_{dm}/K_{ds} were found to be less than 1 for all cases, suggesting that the adsorption of heavy metal ions in the multiple system were reduced through competition for adsorption sites on the zeolite. Moreover, at higher concentration, the values of K_{dm}/K_{ds} lead to a slight decrease, implying that the behaviors of competitive adsorption were stronger at lower concentration.

Treatment of industrial wastewater using zeolite

Based on the results of the heavy metal removal efficiency from aqueous solutions, tests were conducted to evaluate these results using industrial wastewaters, including desulfurization wastewater from wet limestone-gypsum system and metal plating wastewater from local metal plating factory. The desulfurization wastewater had a pH of 4.2 and contained 8.4 mg/L of Cd²⁺, 1.82 mg/L of Pb²⁺, 5.7 mg/L of Mn²⁺, 4.6 mg/L of Ni²⁺, and 7.5 mg/L of Cu²⁺. The metal plating wastewater had a pH of 2.7 and contained 103 mg/L of Ni²⁺ and 45 mg/L of Cu²⁺. The pH of the wastewaters was adjusted to

4.0, and the tests were conducted with varying zeolite dosage. The results were presented in Fig. 9a, b, respectively.

It can be observed that the heavy metals' removal efficiency increased when the zeolite dosage increased. The optimum zeolite dosage for heavy metals removal is 4 g/L for desulfurization wastewater with the removal efficiencies of 93±1.1, 95±0.7, 94±0.6, 85±0.5, and 78±0.7 % for Pb²⁺, Cu²⁺, Cd²⁺, Ni²⁺, and Mn²⁺, respectively. The optimum zeolite dose for heavy metals removal is 15 g/L for metal plating wastewater and the removal efficiencies were 95±2.0 and 98±0.5 % for Ni²⁺ and Cu²⁺, respectively. The results demonstrated that

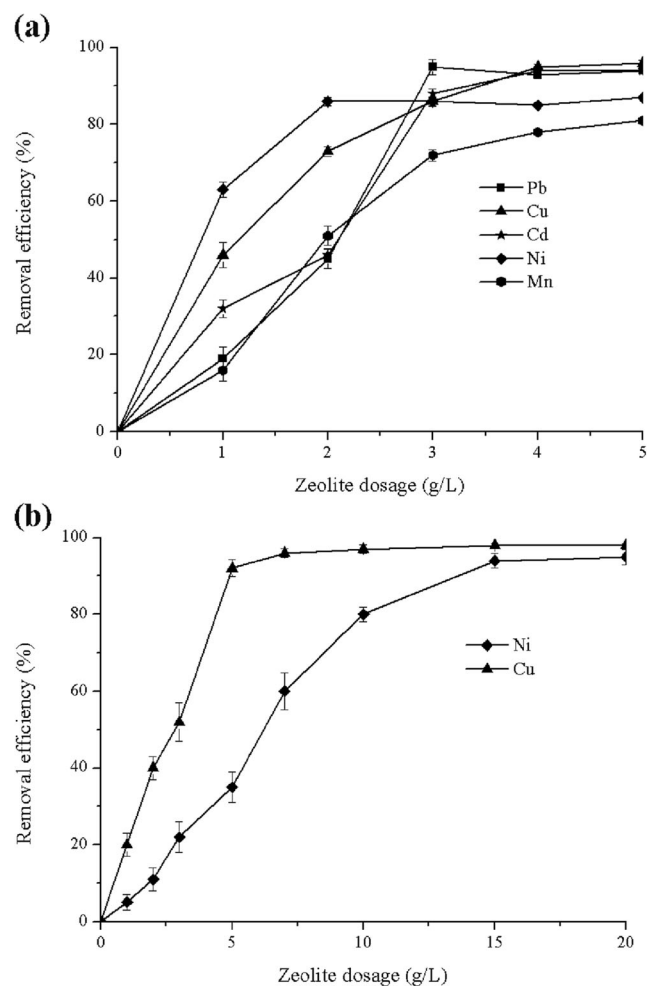


Fig. 9 Effect of adsorbent dosage on the removal of heavy metals from wastewater: **a** desulfurization wastewater, **b** metal plating wastewater

zeolite could be used as an effective adsorbent for the removal of heavy metals from industrial wastewater.

Conclusion

In this study, zeolite was synthesized from fly ash, and its heavy metals adsorption capacity was evaluated. Zeolite showed a much higher adsorption capacity than did fly ash, and the removal efficiency of heavy metal was increased with the increasing of adsorbent dosage. The solution pH and coexisting cations could significantly affect the removal efficiency of the heavy metals, and the competition capacity of the cations was in the order of $\text{Al}^{3+} > \text{NH}_4^+ > \text{Ca}^{2+} > \text{Mg}^{2+} > \text{Na}^+$. The experimental data were well fitted by the Langmuir model in both the single and multiple systems and the maximum adsorption capacities for Pb^{2+} , Cu^{2+} , Cd^{2+} , Ni^{2+} , and Mn^{2+} were 65.75, 56.06, 52.12, 34.40, and 30.89 mg/g and 45.28, 32.86, 26.93, 16.25, and 14.63 for the single and multiple systems, respectively. Adsorption behavior of zeolite for heavy metals follows an order of $\text{Pb}^{2+} > \text{Cu}^{2+} > \text{Cd}^{2+} > \text{Ni}^{2+} > \text{Mn}^{2+}$. The adsorption behavior of zeolite was also tested using industrial wastewater and showed that zeolite was effective in the removal of various heavy metals in real wastewater. The results indicated that the coal fly ash-prepared zeolite could be used as an effective adsorbent for the removal of heavy metal ions from aqueous solution.

Acknowledgments The research was financially supported by grants from the Guangdong Province Science and Technology Project (Nos. 2013B090200016 and 2013B021000008), Joint Fund of Guangdong Province (No. U1401235), Major Science and Technology program for the Industry-Academia-Research collaborative Innovation of Guangzhou, and the Electric Power Research Institute of Guangdong Grid Co (No. K-GD2013-0501).

References

- Ahmaruzzaman M (2010) A review on the utilization of fly ash. *Prog Energy Combust Sci* 36(3):327–363
- Ajjabi LC, Chouba L (2009) Biosorption of Cu^{2+} and Zn^{2+} from aqueous solutions by dried marine green macroalga *Chaetomorpha linum*. *J Environ Manage* 90:3485–3489
- Álvarez-Ayuso E, García-Sánchez A, Querol X (2003) Purification of metal electroplating waste waters using zeolites. *Water Res* 37: 485–486
- Álvarez-Ayuso E, Querol X, Plana F, Alastuey A, Moreno N, Izquierdo M, Font O, Moreno T, Díez S, Vázquez E, Barra M (2008) Environmental, physical and structural characterization of geopolymer matrixes synthesized from (co-) combustion fly ashes. *J Hazard Mater* 154:175–183
- Ayoob S, Gupta AK, Bhakat PB, Bhat VT (2008) Investigations on the kinetics and mechanisms of sorptive removal of fluoride from water using alumina cement granules. *Chem Eng J* 140:6–14
- Balsamo M, Natale FD, Erot A, Lancia A, Montagnaro F, Santoro L (2011) Cadmium adsorption by coal combustion ashes-based sorbents-relationship between sorbent properties and adsorption capacity. *J Hazard Mater* 187:371–378
- Bandura L, Franus M, Jozefaciuk G, Franus W (2015) Synthetic zeolites from fly ash as effective mineral sorbents for land-based petroleum spills cleanup. *Fuel* 147:100–107
- Barczak M, Michalak-Zwierz K, Gdula K, Tyszczyk-Rotko K, Dobrowolski R, Nbrowski A (2015) Ordered mesoporous carbons as effective sorbents for removal of heavy metal ions. *Microporous Mesoporous Mater* 211:162–173
- Bayat B (2002) Comparative study of adsorption properties of Turkish fly ashes II. The case of chromium (VI) and cadmium (II). *J Hazard Mater B95*:275–290
- Boujelben N, Bouzid J, Elouear Z (2009) Adsorption of nickel and copper onto natural iron oxide-coated sand from aqueous solutions: study in single and binary systems. *J Hazard Mater* 163:376–382
- Bukhari SS, Behin J, Kazemian H, Rohani S (2015) Conversion of coal fly ash to zeolite utilizing microwave and ultrasound energies: a review. *Fuel* 140:250–266
- Calvo B, Canoira L, Morante F, Martínez-Bedia JM, Vinagre C, García-González JE, Elsen J, Alcantara R (2009) Continuous elimination of Pb^{2+} , Cu^{2+} , Zn^{2+} , H^+ and NH_4^+ from acidic waters by ionic exchange on natural zeolites. *J Hazard Mater* 166:619–627
- Cho H, Oh D, Kim K (2005) A study on removal characteristics of heavy metals from aqueous solution by fly ash. *J Hazard Mater B127*:187–195
- Covelo EF, Andrade ML, Vega FA (2004) Heavy metal adsorption by humic umbrilsols: selectivity sequences and competitive sorption kinetics. *J Colloid Interface Sci* 280:1–8
- Franus W, Wdowin M, Franus M (2014) Synthesis and characterization of zeolites prepared from industrial fly ash. *Environ Monit Assess* 186:5721–5729
- Fu FL, Wang Q (2011) Removal of heavy metal ions from wastewaters: a review. *J Environ Manage* 92:407–418
- Höller H, Wirshing U (1985) Zeolite formation from fly ash. *Fortschr Mineral* 63:21–43
- Hollman GG, Steenbruggen G, Janssen-Jurkovicova M (1999) A two-step process for the synthesis of zeolites from coal fly ash. *Fuel* 78: 1225–1230
- Huang Y, Han M (2011) The influence of $\alpha\text{-Al}_2\text{O}_3$ addition on microstructure, mechanical and formaldehyde adsorption properties of fly ash-based geopolymer products. *J Hazard Mater* 193:90–94
- Hui KS, Chao CYH, Kot SC (2005) Removal of mixed heavy metal ions in wastewater by zeolite 4A and residual products from recycled coal fly ash. *J Hazard Mater B127*:89–101
- Inglezakis VJ, Loizidou MD, Grigoropoulou HP (2002) Equilibrium and kinetic ion exchange studies of Pb^{2+} , Cr^{3+} , Fe^{3+} and Cu^{2+} on natural clinoptilolite. *Water Res* 36:2784–2792
- Izidorio JDC, Fungaro DA, Abbott JE, Wang SB (2013) Synthesis of zeolites X and A from fly ashes for cadmium and zinc removal from aqueous solutions in single and binary ion systems. *Fuel* 103:827–834
- Karnib M, Kabbani A, Holail H, Olama Z (2014) Heavy metals removal using activated carbon, silica and silica activated carbon composite. *Energy Procedia* 50:113–120
- Kyziol-Komosinska J, Rosik-Dulewska C, Franus M, Antoszczyszyn-Szpicka P, Czupiol J, Krzyzewska I (2015) Sorption capacities of natural and synthetic zeolites for $\text{Cu}(\text{II})$ ions. *Pol J Environ Stud* 24: 1111–1123
- Leinonen H, Lehto J (2001) Purification of metal finishing waste waters with zeolites and activated carbons. *Waste Manag Res* 19:45–57
- Li L, Wang SB, Zhu ZH (2006) Geopolymeric adsorbents from fly ash for dye removal from aqueous solution. *J Colloid Interface Sci* 300:52–59
- Majdan M, Pikus S, Kowalska-Temes M, Gladysz-Plaska A, Staszczuk P, Fuks L, Skrzypek H (2003) Equilibrium study of selected divalent d-

- electron metals adsorption on A-type zeolite. *J Colloid Interface Sci* 262:321–330
- Mihaly-Cozmuta L, Mihaly-Cozmuta A, Peter A, Nicula C, Tutu H, Silipas D, Indrea E (2014) Adsorption of heavy metal cations by Na-clinoptilolite: equilibrium and selectivity studies. *J Environ Manage* 137:69–80
- Mohan S, Gandhinathi R (2009) Removal of heavy metal ions from municipal solid waste leachate using coal fly ash as an adsorbent. *J Hazard Mater* 169:351–359
- Ouki SK, Kavannagh M (1997) Performance of natural zeolites for the treatment of mixed metal-contaminated effluents. *Waste Manag Res* 15:383–394
- Padervand M, Gholami MR (2013) Removal of toxic heavy metal ions from waste water by functionalized magnetic core-zeolitic shell nanocomposites as adsorbents. *Environ Sci Pollut Res* 20:3900–3909
- Prakash N, Sudha PN, Renganathan NG (2012) Copper and cadmium removal from synthetic industrial wastewater using chitosan and nylon 6. *Environ Sci Pollut Res* 19:2930–2941
- Querol X, Umaña JC, Plana F, Alastuey A, Lopez-Soler A, Medinaceli A, Valero A, Domingo MJ, Garcia-Rojo E (2001) Synthesis of zeolites from fly ash at pilot plant scale. Examples of potential applications. *Fuel* 80:857–865
- Semmens MJ, Seyfarth M (1978) The selectivity of clinoptilolite for certain heavy metals. In: Sand LB, Mumpton FA (eds) *Natural zeolites: occurrence, properties, use*. Pergamon Press Ltd, Oxford, pp 517–526
- Shi LN, Zhou Y, Chen ZL, Megharaj M, Naidu R (2013) Simultaneous adsorption and degradation of Zn^{2+} and Cu^{2+} from wastewater using nanoscale zero-valent iron impregnated with clays. *Environ Sci Pollut Res* 20:3639–3648
- Shigemoto N, Sugiyama S, Hayashi H (1995) Characterization of Na-X, Na-A, and coal fly ash zeolites and their amorphous precursors by IR, MAS NMR and XPS. *J Mater Sci* 30:5777–5783
- Somerset VS, Petrik LF, White RA, Klink MJ, Key D, Iwuoha EI (2005) Alkaline hydrothermal zeolites synthesized from high SiO_2 and Al_2O_3 co-disposal fly ash filtrates. *Fuel* 84:2324–2329
- Sprynsky M, Buszewski B, Terzyk AP, Namiesnik J (2006) Study of the selection mechanism of heavy metal (Pb^{2+} , Cu^{2+} , Ni^{2+} , and Cd^{2+}) adsorption on clinoptilolite. *J Colloid Interface Sci* 304:21–28
- Vega FA, Covelo EF, Andrade ML (2006) Competitive sorption and desorption of heavy metals in mine soils: influence of mine soil characteristics. *J Colloid Interface Sci* 298:582–592
- Volkov AG, Paula S, Deamer DW (1997) Two mechanisms of permeation of small neutral molecules and hydrated ions across phospholipid bilayers. *Bioelectrochem Bioenerg* 42:153–160
- Wang SB, Lin L, Zhu ZH (2007) Solid-state conversion of fly ash to effective adsorbents for Cu removal from wastewater. *J Hazard Mater* B139:254–259
- Wang SB, Ma Q, Zhu ZH (2008) Characteristics of coal fly ash and adsorption application. *Fuel* 87:3469–3473
- Wdowin M, Franus M, Panek R, Badura L, Franus W (2014) The conversion technology of fly ash into zeolites. *Clean Techn Environ Policy* 16:1217–1223
- Wen Y, Tang ZR, Chen Y, Gu YX (2011) Adsorption of Cr (VI) from aqueous solutions using chitosan-coated fly ash composite as biosorbent. *Chem Eng J* 175:110–116
- Wu DY, Sui YM, He SB, Wang XZ, Cj L, Kong HN (2008) Removal of trivalent chromium from aqueous solution by zeolite synthesized from coal fly ash. *J Hazard Mater* 155:415–423
- Xu XT, Li Q, Cui H, Pang JF, Sun L, An H, Zhai JP (2010) Adsorption of fluoride from aqueous solution on magnesia-loaded fly ash cenospheres. *Desalination* 272:233–29
- Xu XY, Cao XD, Zhao L, Wang HL, Yu H, Gao B (2013) Removal of Cu, Zn and Cd from aqueous solutions by the dairy manure-derived biochar. *Environ Sci Pollut Res* 20:358–368
- Yaday S, Srivastava V, Banerjee S, Gode F, Sharma YC (2013) Studies on the removal of nickel from aqueous solutions using modified riverbed sand. *Environ Sci Pollut Res* 20:558–567
- Zhan YH, Lin JW, Li J (2013) Preparation and characterization of surfactant-modified hydroxyapatite/zeolite composite and its adsorption behavior toward humic acid and copper (II). *Environ Sci Pollut Res* 20:2512–2526